Low-frequency vibration measurement by temporal analysis of projected fringe patterns

Yu Fu

Department of Mechanical Engineering, National University of Singapore,
9 Engineering Drive 1, Singapore 117576, Singapore

Abstract

Fringe projection is a whole field, non-contacting optical technique allowing direct measurement of surface contour of an object. In many cases, 3D surface profiling is required for vibrating objects or for objects with continuously changing profile, where conventional phase shifting techniques are not applicable. Carrier-based spatial Fourier, window Fourier analyses, or wavelet analysis are normally used to retrieve instantaneous phase maps in dynamic measurement from one fringe pattern, but these techniques require high-quality surface, such as uniform reflectivity, continuity of the surface and a regular shape. Otherwise, large errors will be generated during the process. In this study, a grating is projected on the surface of a low-frequency vibrating object and a sequence of fringe patterns is captured by a high-speed camera. The fringe patterns are processed point-by-point along time axis by different algorithms. To avoid the phase ambiguity problem, a temporal carrier is introduced in the experiment by shifting the grating with a constant speed. The results show that high-quality instantaneous surface profile and the kinematic parameters of vibration, such as displacement, velocity and acceleration can be obtained precisely.

Keywords: Fringe projection; Fourier analysis; windowed Fourier analysis; vibration measurement; phase retrieval; temporal carrier.

1. Introduction

Optical techniques are widely used to determine three-dimensional profile and measurement of vibration in many engineering fields [1-5]. Generally they are non-contact and non-destructive and are desirable for vibration analysis, quality control and contouring mapping. Among them, the fringe projection method [6] is gaining grounds in many engineering applications, such as dimension measurement for die development, stamping panel geometry checking [7], etc. Recently, it has also been extended to the measurement of micro-components such as MEMS structure [8]. In fringe projection technique, a known optical fringe pattern is projected onto the surface of interest; the distribution of the fringe pattern on the surface is perturbed in accordance with the profile of the test surface, thereby enabling direct derivation of surface profiles. Phase shifting techniques [4,9], combined with a 2D spatial phase unwrapping [10], are usually employed by projecting several fringe patterns with prescribed phase shift; however, it is restricted to static or quasi-static objects. In many cases, instantaneous 3D surface profiling is required for vibrating objects or for objects with continuously changing profile. In addition, the kinematic parameters, such as displacement, velocity and acceleration are also of interest in dynamic measurement [11].

Because of the rapid development of high-speed digital recording devices, it is now possible to record projected fringe pattern with rates exceeding 10,000 frames per second (fps). In order to calculate the phase distribution at each instant, different spatial techniques have been reported to retrieve the phase map from one projected fringe pattern. Huang et al. [12] developed a color-encoded fringe projection technique to calculate the phase map by separating fringes with different colors followed by a phase shifting. However, it is quite difficult to split the color fringes into RGB components due to the overlapping of the spectra. Carrier-based

Fourier transform profilometry [13, 14] is the most popular method to retrieve the phase spatial distribution from one fringe pattern. It requires fringes with high-spatial frequency acting as a carrier. With proper filtering in frequency domain, the contour can also be evaluated. In some cases, it is an effective approach for dynamic measurement [15]. Recently 2D windowed Fourier transform (WFT) [16,17], 1D and 2D continuous wavelet transform (CWT) [18-20] have also been reported to retrieve the phase from one fringe pattern. These spatial techniques require uniform reflectivity and continuity of the surface. In addition, these techniques are based on global or localized matrix manipulation, which will generate large error at the edge of the zero-padding areas. Hence the shape of the object is better to be regular to form an intensity matrix. However, in many cases, these requirements are not easily satisfied.

Temporal phase analysis and temporal phase unwrapping techniques [21-23] were introduced to overcome these problems in the late 1990s. In this technique, a sequence of fringe patterns is recorded throughout the entire deformation history of the object. Each pixel is then analyzed as a function of time. Different algorithms [24-29] have been introduced to retrieve the temporal phase. The Fourier transform (FT) [26] is still the most popular method in temporal analysis. The intensity fluctuation of each pixel is first transformed and one side of the spectrum is filtered with a bandpass filter. The filtered spectrum is inverse transformed to obtain the wrapped phase. The phase values are then unwrapped along the time axis at each pixel independently of other pixels in the image. However, the deformation of each point on the object is different, and the deformation of each pixel may also be non-linear along the time axis. The bandpass filter must be broadened; therefore the efficiency of noise elimination is reduced.

In recent years, WFT and CWT have also been introduced in temporal phase extraction [11,27-29]. Both algorithms can limit the influence of various noise sources and improve the

result in phase extraction. In addition, both techniques can extract the instantaneous frequency of the temporal intensity variation from which the velocity and acceleration of the deformation or vibration can be evaluated. However, previous research [11] has showed that for temporal intensity variation signals, both techniques may generate large errors if the parameters are not properly selected. WFT suffers due to its fixed window size, while CWT sometimes is also not a good choice because of its poor performance at low-frequency part. The best temporal processing algorithm for intensity variation signal is the combination of Fourier and windowed Fourier analysis. In addition, the determination of absolute sign of the phase is impossible by temporal Fourier, WFT and CWT analyses. This limits the techniques to the measurement of deformation in one known direction. Adding a temporal carrier frequency to the image acquisition process is a method to overcome these problems [23,28]. The carrier frequency should be high enough so that the phase change on any point is in one direction.

Based on previous work, this paper proposes a temporal analysis on the measurement of the instantaneous surface contour, out-of-plane displacement, velocity and acceleration of a low-frequency vibrating object in a fringe projection setup. The objects to be measured do not have a regular shape and spatial carrier-based processing may general large errors. A temporal carrier is introduced by projecting a moving grating on the specimen. The phase variation due to temporal carrier can be calibrated in advance. The frequency-modulated (FM) intensity variation signal is then processed by the combination of temporal Fourier and windowed Fourier analysis. After removing the effect of temporal carrier, the absolute instantaneous displacement, velocity and acceleration of a vibrating object are obtained. The comparison among the results of instantaneous profiling of a vibrating coin by different methods is also presented to illustrate the advantages of temporal analysis. On the other hand, the disadvantages of temporal analysis and

temporal carrier are also discussed so that the readers will have a more comprehensive understanding on the selection of proper processing algorithms along different axes in fringe projection technique.

2. Theoretical Analysis

In this section, a brief illustration of fringe projection technique and the different temporal processing algorithms will be presented, followed by an introduction of spatial and temporal carrier in fringe projection technique.

2.1. Fringe projection technique

The schematic layout of the fringe projection and imaging system is shown in Fig. 1. When the object is imaged at right angle, the phase change φ due to height h is given by

$$h = \frac{L}{d} S = \frac{L}{d} \frac{\varphi}{2\pi f_S} = k\varphi, \tag{1}$$

where L is the distance between the projector and the reference plane, d is the distance between the projector and camera axis, f_S is the spatial frequency of the projected fringes on the reference plane and k is an optical coefficient related to the configuration of the system. It varies little when the object is small and the projection beam is collimated. However, a pixel-wise calibration is still necessary for a precise measurement. φ is the phase variation which contains the surface height information.

When a moving sinusoidal grating is projected onto a continuously deforming or vibrating object, the distribution of the grating is perturbed by the vibration or deformation of the specimen and the initial profile of the test surface. The mathematical representation of the

intensity distribution captured by a high-speed CCD camera is governed by the following equation:

$$I(x,y,t) = a(x,y,t) + b(x,y,t)\cos[2\pi f_S x + 2\pi f_C t + \varphi_0(x,y) + \varphi(x,y,t)], \quad (2)$$

where $a(x,y,t)$ and $b(x,y,t)$ are the background and modulation factor, respectively. $\varphi_0(x,y)$ is an initial phase which contains the shape information, f_C is the temporal carrier frequency of the projected fringes, and $\varphi(x,y,t)$ is a time-dependent phase function related to the object vibration or deformation. $a(x,y,t)$ and $b(x,y,t)$ are both slowly varying functions along time axis, which can be considered as a constant in this case. A sequence of intensity value in Eq. (2) forms a 3D matrix which can be processed either in spatial domain (x-y plane) or time domain (t-axis) by following processing algorithms.

2.2. Temporal processing algorithms

2.2.1. Fourier transform

Fourier transform and inverse Fourier transform are widely used in filtering and phase extraction. The Fourier transform of a one-dimensional intensity variation signal $I(t)$ can be expressed as:

$$\hat{I}(\xi) = \int_{-\infty}^{+\infty} I(t)\exp(-j\xi t)\,dt, \quad (3)$$

where $\hat{I}(\xi)$ is the Fourier transform of $I(t)$. The Fourier spectrum is filtered by a bandpass filter, and the inverse Fourier transform yields an exponential signal $C(t)$ from which the phase can be calculated by

$$\Phi(t) = \varphi_C(t) + \varphi(t) = \arctan\frac{\mathrm{Im}\left(C(t)\right)}{\mathrm{Re}\left(C(t)\right)} \tag{4}$$

where Re and Im denote the real and imaginary parts of $C(t)$, respectively. $\varphi_C(t)$ is the phase variation of temporal carrier which can be pre-calibrated and removed. The phase obtained is wrapped between $-\pi$ to $+\pi$. A 1D temporal unwrapping procedure is needed to reconstruct the continuous phase function $\Phi(t)$.

It is well known that the accuracy of the phase extraction based on FT analysis increases with the decrease of the width of the bandpass filter. However, when the phase change of the signal is highly non-linear, the width of the sideband in the spectrum increases. In dynamic measurements it occurs quite often as the velocity of the object is normally varying. In addition, different pixels have different spectra when the object is subjected to a non-rigid-body vibration or deformation. Hence, the selection of a proper window size for bandpass filtering for all pixels becomes difficult. Normally a relatively large filtering window is selected. This means that noise whose frequency is within the filtering windows cannot be removed by Fourier transform. This problem can be overcome by using a windowed Fourier transform.

2.2.2. Windowed Fourier transform

A one-dimensional windowed Fourier transform of a temporal signal $I(t)$ can be written as [30]

$$SI(u,\xi) = \int_{-\infty}^{+\infty} I(t) g_{u,\xi}^{*}(t)\, dt \tag{5}$$

where $I(t)$ is the original intensity variation signal, $SI(u,\xi)$ denotes the spectrum of WFT and $g_{u,\xi}(t)$ is the WFT kernel, which can be expressed as

$$g_{u,\xi}(t) = g(t-u)\exp(j\xi t) \tag{6}$$

The window $g(t)$ is usually chosen as the Gaussian function

$$g(t) = \exp\left(-t^2/2\sigma^2\right) \tag{7}$$

which gives the best time-frequency localization in analysis. σ is a parameter to control the expansion of the window size. The instantaneous frequency of the signal $\xi(u) = \varphi'(u)$ can be obtained by extracting the 'ridge' on the spectrum of WFT [11]. A filtered signal phase can be obtained by integration or by extracting the phase on the ridge. It is noteworthy that for an intensity varying signal, the direct use of a WFT may generate a large error because of the effect of DC term and negative frequency [11].

A windowed Fourier transform maps a 1D temporal signal to a 2D time-frequency plane, and extracts the signal's instantaneous frequency. Hence, it is more effective to remove the noise within the frequency band of the signal. However, the time-frequency uncertainty principle affects the resolution, which leads to trade-off between time and frequency localization. The narrower the time window, the better the temporal resolution at the cost of a poorer resolution in frequency and vice versa. However, once the window size is determined, the resolution at different frequencies is also uniform. In WFT, the signal phase is assumed to be linear in the area covered by the Gaussian window. However, in many cases of temporal analysis the signal

frequency varies dramatically. In addition, the temporal signal of fringe projection technique is not very noisy. Hence the window size should be small in order to reduce the linear phase approximation error. It is worth noting that windowed Fourier kernel with a small window size in time will have large window size in the spectrum. When the low frequency part of the signal is processed, the result will be seriously affected by the DC term. Previous research [11] shows a combination of FT and WFT gives a better result as the DC and negative frequency term are removed by a bandpass filter in FT.

2.2.3. Continuous wavelet transform

Continuous wavelet transform is similar to windowed Fourier transform, but with a varying Gaussian window size according to the signal frequency. The details of wavelet transform are illustrated in Ref. [30]. In the wavelet transform, the influence of the DC term can be ignored when the central frequency of the wavelet is more than 5. However, the wavelet transform performs poorly when the signal frequency is low, as it will automatically adjust the window size to be very large in time axis, sometimes even larger than the signal length. This will generate large errors in the phase extraction [11]. Normally a wavelet transform only performs well when the signal frequency is high in fringe analysis.

2.3. Spatial carrier vs. temporal carrier

All the algorithms mentioned above have the phase ambiguity problem. This limits the technique to the phase extraction in one direction which is already known. In fringe projection technique, the carrier already exists in spatial domain. However, the result of spatial processing will be seriously affected by a non-uniform reflectivity of the surface or a height step on the

surface. Zero-padding is also needed for a irregular shape to form a matrix. This will also generate large error at the edge. Fig. 2(a) shows a projected fringe pattern on a cantilever beam with irregular shape. Fig. 2(b) and (c) shows a wrapped phase map after 2D Fourier transform and phase distribution after unwrapping and carrier removal. It can be observed that the phase distortion near the edge is obvious due to the zero-padding area. The results of spatial WFT and CWT are worse due to their lower resolutions in spatial and frequency domain. This example shows that spatial processing may not be a good choice in many cases.

In dynamic measurement by fringe projection technique, introducing a temporal carrier is another option to avoid the phase ambiguity problem. In this application, the temporal carrier is generated by projecting a moving grating on the vibrating specimen. The temporal carrier frequency can be easily controlled by a motorized stage. The combination of Fourier and windowed Fourier analyses is still adopted to extract the phase and the phase derivatives in time axis. The details will be illustrated in the next two sections.

3. Experimental Illustration

Fig. 3 shows the schematic layout of the experimental setup. A commercialized sinusoidal grating with a pitch of 150 line/inch is shifted by a motorized long-travel linear stage (Melles Griot 17 NST 104) with a constant speed of 3.33 mm/s. The moving fringe pattern is projected on specimen by an imaging lens. Two specimens with diffuse surface are measured in this application. One is a cantilever beam as shown in Fig. 3(b). The cantilever beam is fixed at the right-hand side and vibrated at the left-hand side by a shaker (Gearing & Watson, Type 4) connected with a function generator (BK PRECISION 3011B 2MHz). The beam is subjected to a sinusoidal wave vibration with a frequency of approximately 2.4 Hz. Four hundred fringe

patterns were captured at right angle by a high-speed CCD camera (KODAK Motion Corder Analyzer, SR-Ultra) with a recording rate of 250 frame/s (fps). The imaging area (shown in Fig. 3(b)) contains 460×100 pixels and has a length and width of 45 and 9.8 mm, respectively. Four hundred images are recorded within a 1.6s period. In order to present the result of instantaneous surface profiling, a 20-cents Singapore coin is also subjected to a rigid-body vibration and measured by the proposed method.

Several considerations are noteworthy when the proposed experimental setup is designed: (1) The selection of grating pitch is related to several factors:

- Height step on the object;
- Frequency and amplitude of the vibration;
- Measurement sensitivity to be achieved;
- Magnification of projection system;
- Speed and resolution of the translating stage; and
- Capturing rate of high-speed camera.

These factors have to be considered together when a suitable grating is selected. (2) Recent years LCD projector has been widely used in Fringe projection techniques [31]. In this study, two conditions should be satisfied if a LCD projector is applied:

- The response time of LCD projector should be short enough; and
- The LCD projector should be synchronized with the high-speed camera so that there is a certain amount of phase shift between two adjacent fringe patterns.

However, these two conditions are not easily satisfied by a commercialized LCD projector, especially when the capturing rate of the high-speed camera is high.

4. Results and discussion

Fig. 4(a) shows the intensity variation on point A [indicated in Fig. 3(b)]. It is a frequency-modulated signal and the frequency band depends on the velocity and amplitude of the vibration. Fig. 4(b) shows the phase variation of point A after temporal Fourier analysis. After removal of the temporal carrier, the absolute phase variation due to vibration can be obtained as shown in Fig. 4(c). In order to remove the obvious noise and extract the first derivative of the phase, the phase variation $\varphi(t)$ is converted to an exponential signal $\exp\left(j\cdot\varphi(t)\right)$. Windowed Fourier ridge method [11] is then applied. Fig. 4(d) and (e) shows the phase and its first derivative which are proportional to the displacement and velocity, respectively. Similarly WFT ridge method can also be applied on the signal of $\exp\left(j\cdot\varphi(t_n)\right)\cdot\exp\left(-j\cdot\varphi(t_{n-1})\right)$ so the second derivative of the phase (Fig. 4(f)) can also be extracted. At a certain instant, the displacement, velocity and acceleration distribution can be obtained by a combination of phase values on each pixel. Fig. 5(a) and (b) are the phase distribution at frame No. 100 which is proportional to the displacement by temporal Fourier and temporal WFT analyses, respectively. As the signal is not so noisy, $\sigma = 3$ is selected as a window size to limit the linear phase approximation error. It can be observed the result from WFT is better than that from Fourier analysis. The WFT results of velocity and acceleration distribution at frame No. 100 are shown in Fig. 6(a) and (b), respectively. Without any spatial filtering, a good quality distribution of three kinematic parameters is obtained by the proposed method. The relative errors of displacement, velocity and acceleration measurement are 1%, 2% and 7%, respectively [29].

In fringe projection technique, the instantaneous surface profile of a vibrating object can also be extracted by temporal analysis followed by a 2D phase unwrapping. In order to compare the result of surface profiling, a 20-cent Singapore coin is subjected to a low-frequency rigid-

body vibration. The setup is same as the previous experiment. Fig. 7(a) shows a typical fringe pattern. The phase map produced by 2D spatial Fourier analysis is shown in Fig. 7(b). The result is in low quality and the edge effect is obvious. Fig. 7(c) shows a phase map produced by a static measurement using conventional 4-step temporal phase shifting. A periodic ripple appears in the result. It is caused by the inherent limitation of the phase shifting algorithm [18]. In this application, the ripple is of the same order as the profile, which is not acceptable. Fig. 7(d) shows the instantaneous surface profile from temporal Fourier analysis. Ripple effect [32] still be observed, but the result is better compared to phase shifting technique. Fig. 7(e) shows the result of temporal WFT analysis based on FT result. Fig. 7(f) shows the results from temporal CWT analysis of the initial intensity variation signal. In this application, the CWT produces the similar result as the combination of Fourier and windowed Fourier analyses, as the signal frequencies are in a high level and the window size of CWT are quite small in time domain. The linear approximation error can be ignored. However, the combination of Fourier and windowed Fourier analyses is still recommended in the temporal analysis of intensity variation signal [11] when the signal frequency is low.

It can be observed that temporal analysis generally produces better results in dynamic measurement, while spatial analysis results depends on the shape and surface reflectivity of the specimen. However, temporal analysis can only be applied in the cases that the in-plane displacement can be ignored. In addition, introducing a temporal carrier sometimes is not easily accomplished in the experiment. The temporal carrier frequency also limits the measurement range of phase variation due to the constraints of Nyquist sampling theorem and the acquisition speed of the high-speed camera [28]. A comprehensive consideration is needed on the selection

of proper processing algorithms along different axes in the dynamic measurement by fringe projection technique.

5. Concluding remarks

In this paper, a novel method for evaluating the transient surface profile, displacement, velocity and acceleration of a vibrating object is presented based on fringe projection technique. In order to overcome the phase ambiguity problem, a temporal carrier is introduced by projecting a moving grating on the vibrating object. The carrier frequency should be high enough to ensure the phase change of each point is in one direction. Different temporal analysis algorithms are compared on two specimens. A combination of Fourier and windowed Fourier transform is recommended in temporal phase analysis. The results show that the fringe projection and temporal analysis allow the simultaneous evaluation of surface profile and three important vibration parameters of a low-frequency vibrating object at different instants by a whole-field non-contact optical technique.

References

1. Harding KG, Harris JS. Projection moiré interferometer for vibration analysis. Appl Opt 1983; 22:856-61.
2. Prakash S, Upadhyay S, Shakher C. Real-time out-of-plane vibration measurement/monitoring using Talbot interferometry. Opt Laser Eng 2000; 33(4):251-9.
3. Rodriguez-Vera R, Kerr D, Mendoza-Santoyo F. 3-D contouring of diffuse objects by Talbot-projected fringes. J Mod Opt 1991; 38(10): 1935-45.
4. Dirckx JJJ, Decraemer WF. Phase shift moiré apparatus for automatic 3D surface measurement. Rev Sci Instrum 1989; 60(12): 3698-701.
5. Reid GT, Rixon RC, Messer HI. Absolute and comparative measurements of three-dimensional shape by phase measuring moiré topography. Opt Laser Technol 1984; 16:315-9.
6. Suganuma M, Yoshizawa T. Three-dimensional shape analysis by use of a projected grating image. Opt Eng 1991; 30(10): 1529-33.
7. Chen F, Brown GM, Song M. Overview of three-dimensional shape measurement using optical methods. Opt Eng 2000; 39(1): 10-22.
8. He XY, Kang X, Quan C, Tay CJ, Wang SH, Shang HM. Optical methods for the measurement of MEMS materials and structures. Proc SPIE 2001; 4537: 63-8.
9. Quan C, He XY, Tay CJ, Shang HM. 3D surface profile measurement using LCD fringe projection. Proc SPIE 2001; 4317: 511-6.
10. Ghiglia DC, Pritt MD. Two-dimensional phase unwrapping, theory, algorithms, and software. New York: Wiley; 1998.
11. Fu Y, Groves RM, Pedrini G, Osten W. Kinematic and deformation parameter measurement by spatiotemporal analysis of an interferogram sequence. Appl Opt 2007; 46:8645-55.

12. Huang PS, Hu Q, Jin F, Chiang FP. Color-encoded digital fringe projection for high-speed three-dimensional surface contouring. Opt Eng 1999; 38(6): 1065-71.
13. Su X, Chen W. Fourier transform profilometry: a review. Opt Laser Eng 2001; 35(5): 263-84.
14. Takeda M, Ina H, Kobayashi S. Fourier-transform method of fringe-pattern analysis for computer-based topography and interferometry. J Opt Soc Am 1982; 72: 156-60.
15. Tay CJ, Quan C, Shang HM, Wu T, Wang SH. New method for measuring dynamic response of small components by fringe projection. Opt Eng 2003; 42(6): 1715-20.
16. Qian K. Two-dimensional windowed Fourier transform for fringe pattern analysis: principles, applications and implementations. Opt Laser Eng 2007; 45: 304-17.
17. Qian K, Fu Y, Liu Q, Seah HS, Asundi A. Generalized three-dimensional windowed Fourier transform for fringe analysis. Opt Lett 2006; 31: 2121-3.
18. Miao H, Quan C, Tay CJ, Fu Y. Analysis of phase distortion in phase-shifted fringe projection. Opt Laser Eng 2007; 45(2):318-25.
19. Watkins LR, Tan SM, Barnes TH. Determination of interferometer phase distributions by use of wavelets. Opt Lett 1999; 24: 905-7.
20. Abid AZ, Gdeisat MA, Burton DR, Lalor MJ, Lilley F. Spatial fringe pattern analysis using the two-dimensional continuous wavelet transform employing a cost function. Appl Opt 2007; 46(24): 6120-6.
21. Joenathan C, Franze B, Haible P, Tiziani HJ. Speckle interferometry with temporal phase evaluation for measuring large-object deformation. Appl Opt 1998; 37(13): 2608-14.
22. Huntley JM, Saldner H. Temporal phase-unwrapping algorithm for automated interferogram analysis. Appl Opt 1993; 32: 3047-52.

23. Kaufmann GH. Phase measurement in temporal speckle pattern interferometry using the Fourier transform method with and without a temporal carrier. Opt Commun 2003; 217: 141-9.

24. Li X, Tao G, Yang Y. Continual deformation analysis with scanning phase method and time sequence phase method in temporal speckle pattern interferometry. Opt Laser Technol 2001; 33: 53-9.

25. Tay CJ, Quan C, Fu Y, Chen LJ, Shang HM. Surface profile measurement of low-frequency vibrating objects using temporal analysis of fringe pattern. Opt Laser Technol 2004; 36(6): 471-6.

26. Pawlowski ME, Kujawinska M, Wegiel MG. Shape and motion measurement of time-varying three-dimensional objects based on spatiotemporal fringe-pattern analysis. Opt Eng 2002; 41(2): 450-9.

27. Fu Y, Tay CJ, Quan C, Chen LJ. Temporal wavelet analysis for deformation and velocity measurement in speckle interferometry. Opt Eng 2004; 43(11): 2780-7.

28. Fu Y, Tay CJ, Quan C, Miao H. Wavelet analysis of speckle patterns with a temporal carrier, Appl Opt 2005; 44(6): 959-65.

29. Fu Y, Pedrini G, Osten W. Vibration measurement by temporal Fourier analyses of digital hologram sequence. Appl Opt 2007; 46: 5719-27.

30. Mallat S. A wavelet tour of signal processing. 2nd ed. San Diego: Academic Press; 1999.

31. Buytaert JAN. Dirckx JJJ. Moiré profilometry using liquid crystals for projection and demodulation. Opt Express 2008; 16(1)：179-93.

32. Pan B, Qian K, Huang L, Asundi A. Phase error analysis and compensation for nonsinusoidal waveforms in phase-shifting digital fringe projection profilometry. Opt Lett 2009; 34(4): 416-8.

List of figures

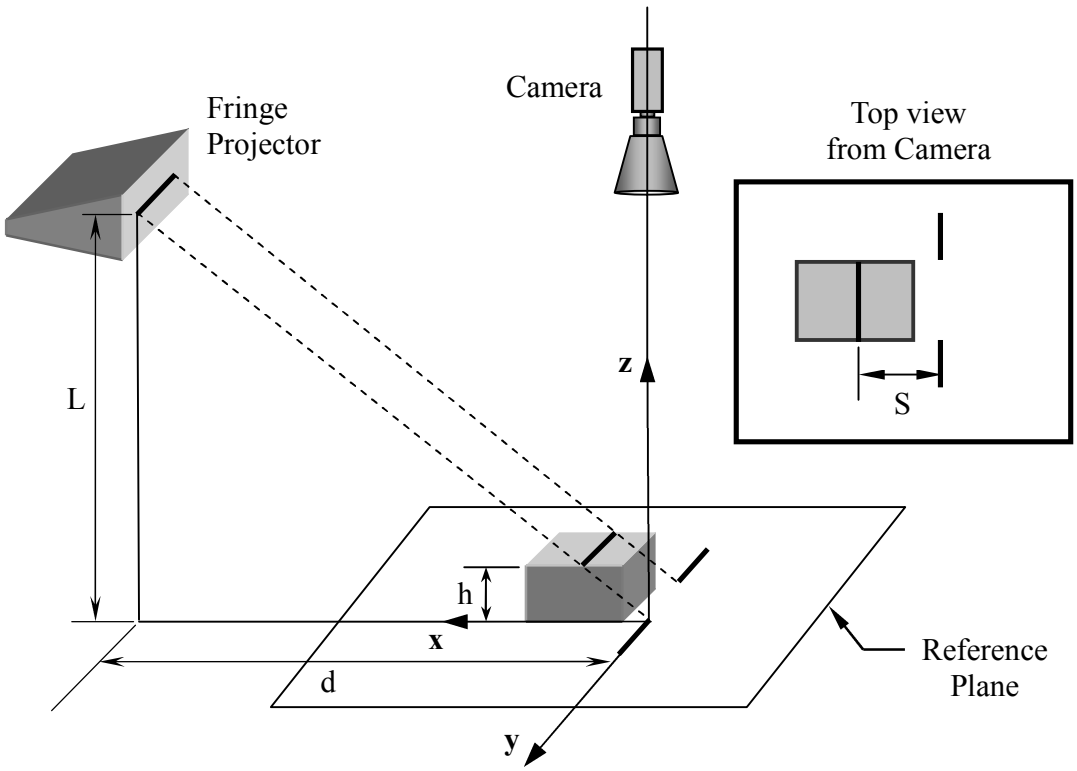
Fringe
Projector
Camera
Top view
from Camera
z
L
S
h
x
d
y
Reference
Plane

Figure 1

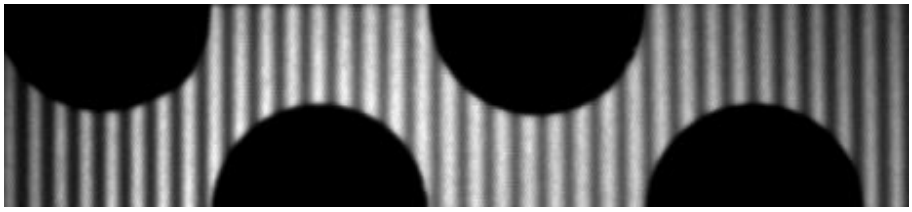

(a)

(b)

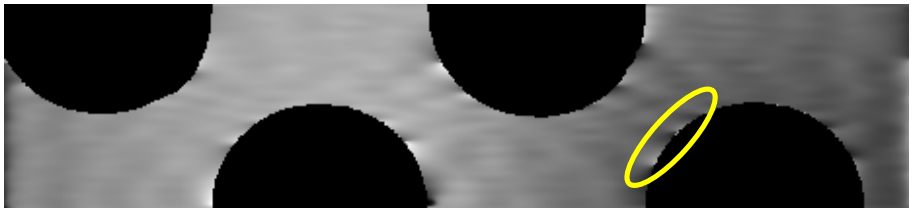

(c)

Figure 2

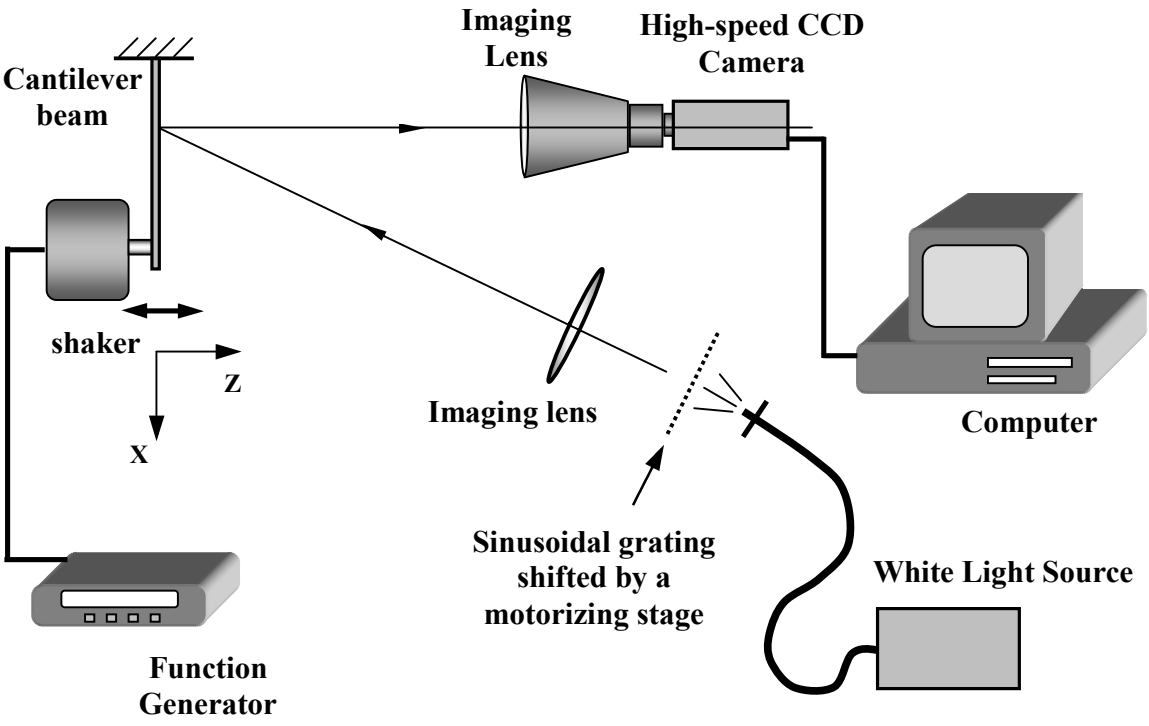
Imaging
Lens
High-speed CCD
Camera
Cantilever
beam
shaker
Z
X
Imaging lens
Computer
Sinusoidal grating
shifted by a
motorizing stage
White Light Source
Function
Generator

(a)

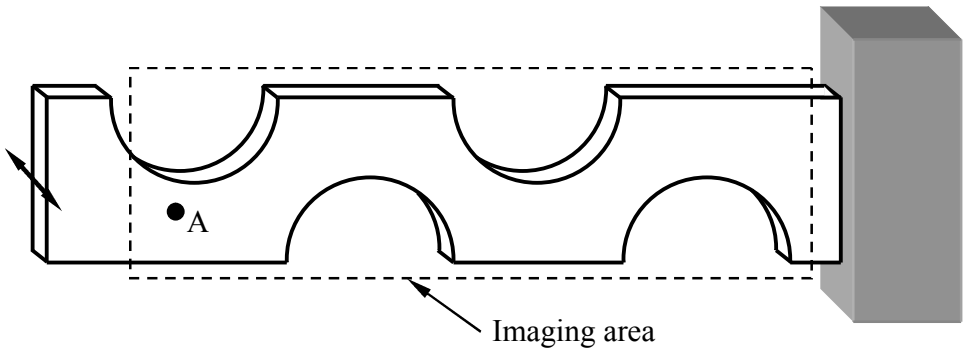
A
Imaging area

(b)

Figure 3

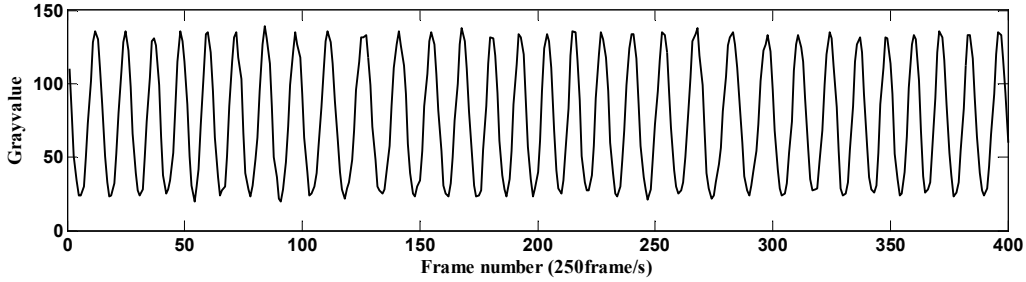
Grayvalue
Frame number (250frame/s)

(a)

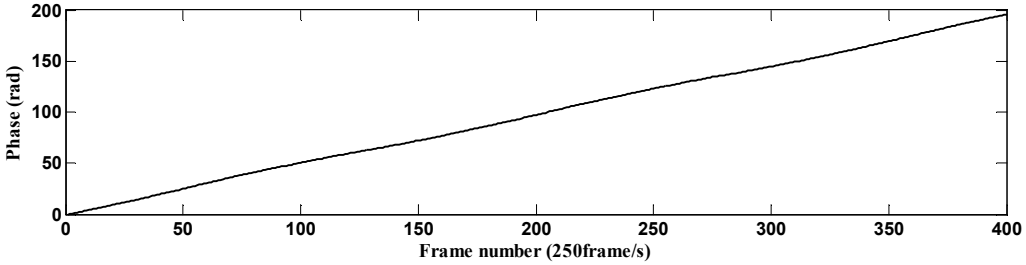
Phase (rad)
Frame number (250frame/s)

(b)

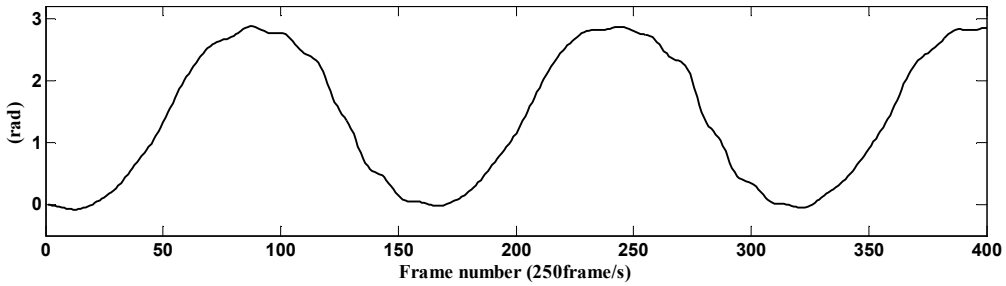
(rad)
Frame number (250frame/s)

(c)

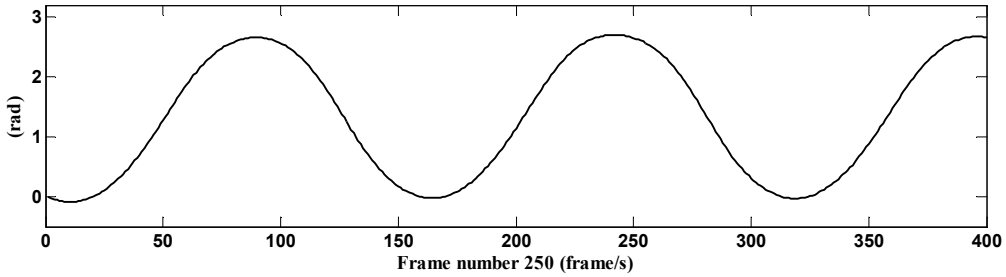
(rad)
Frame number 250 (frame/s)

(d)

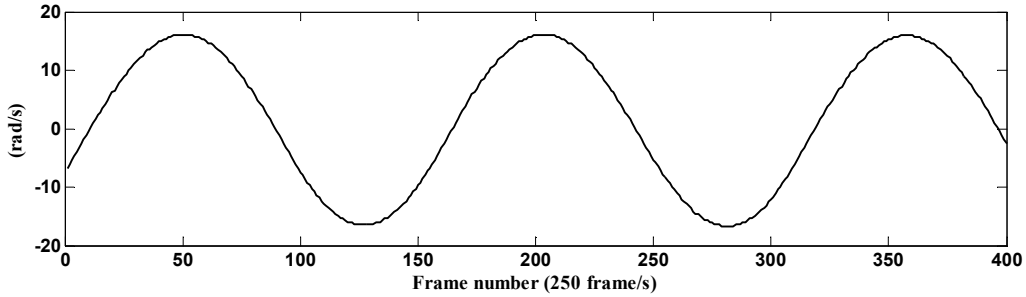
20
10
0
-10
-20
(rad/s)
0
50
100
150
200
250
300
350
400
Frame number (250 frame/s)

(e)

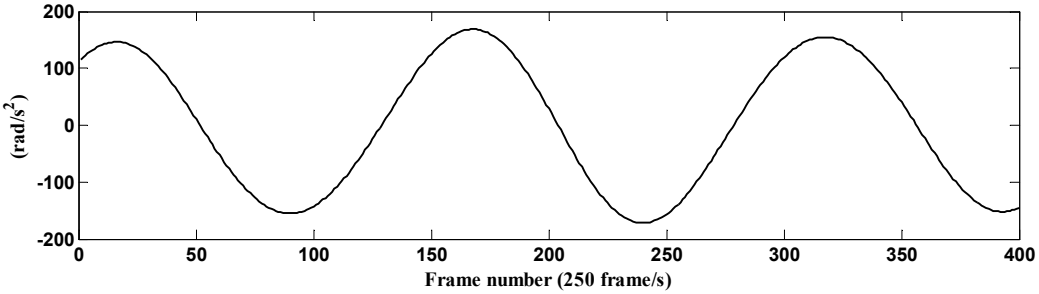
200
100
0
-100
-200
(rad/s^2)
0
50
100
150
200
250
300
350
400
Frame number (250 frame/s)

(f)

Figure 4

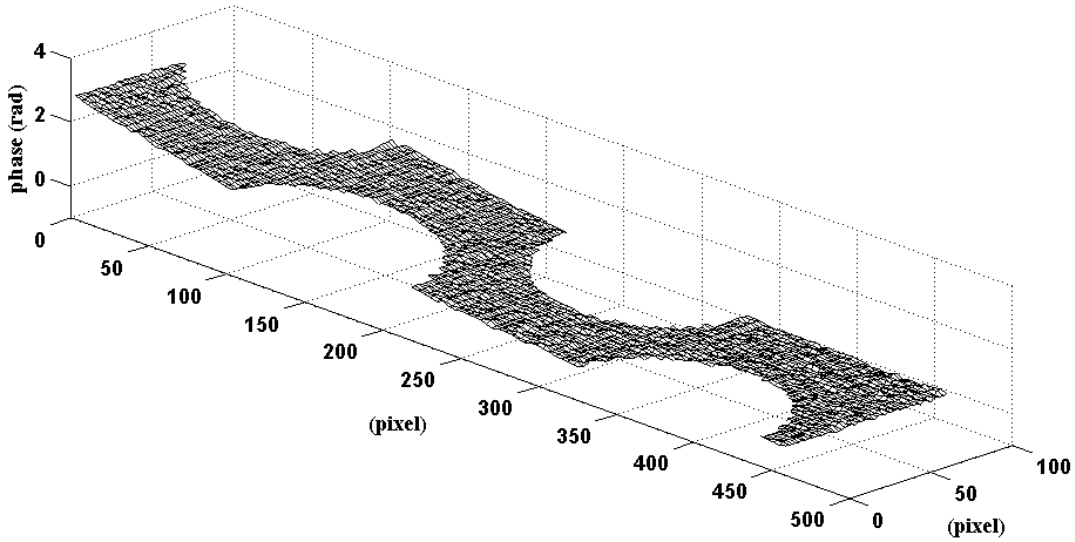
phase (rad)
4
2
0
0
50
100
150
200
250
300
350
400
450
500
(pixel)
0
50
100
(pixel)

(a)

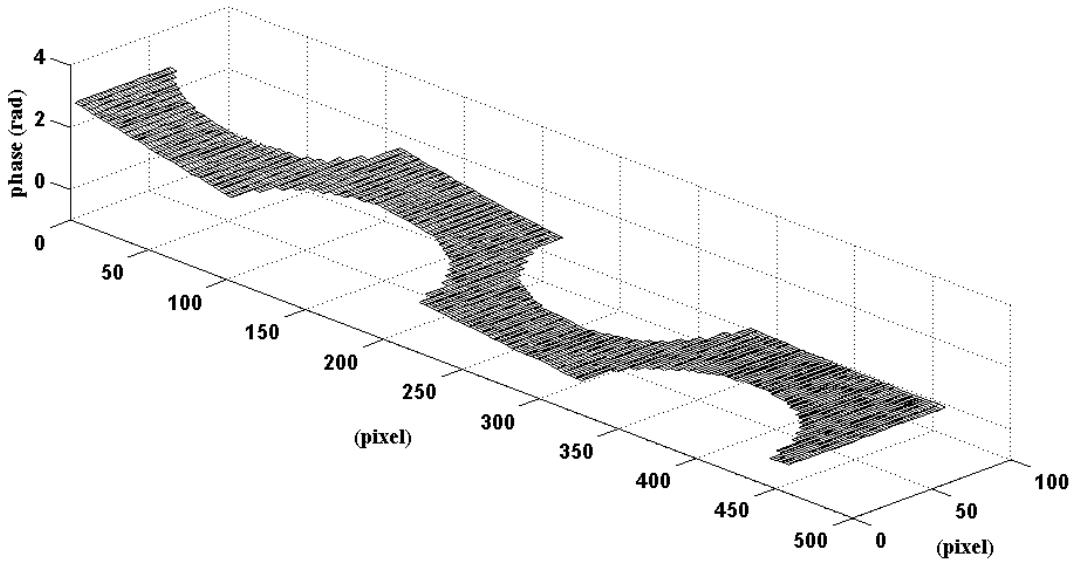
phase (rad)
4
2
0
0
50
100
150
200
250
300
350
400
450
500
(pixel)
0
50
100
(pixel)

(b)

Figure 5

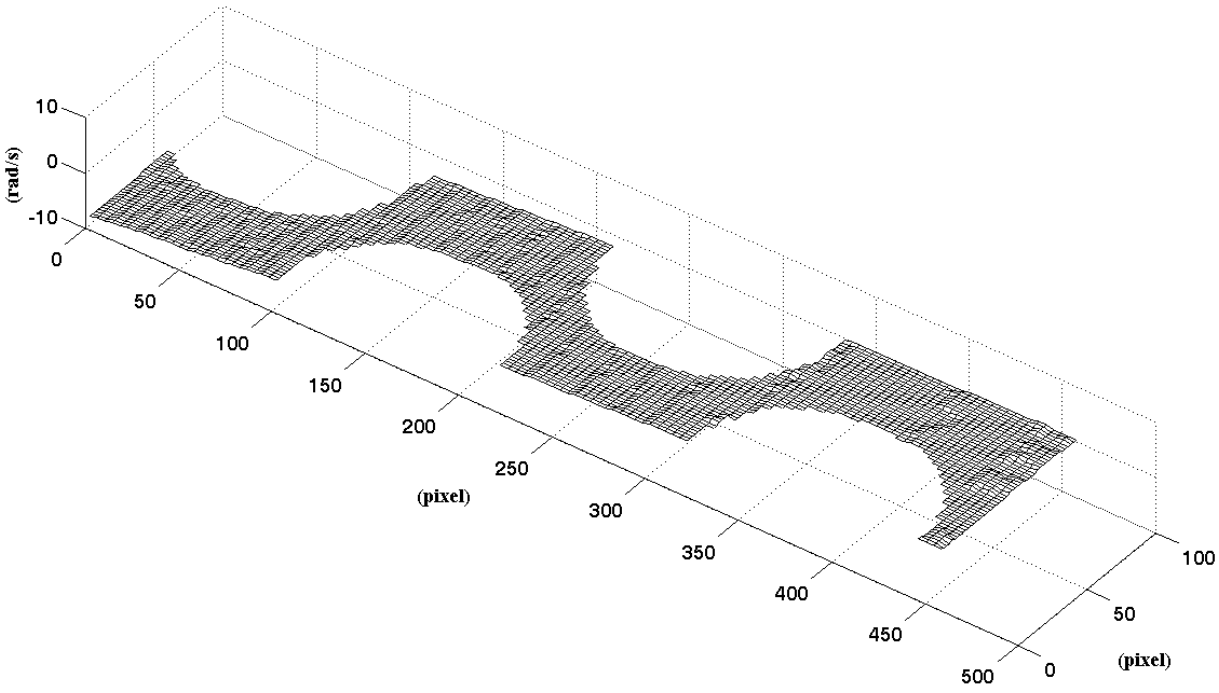
10
0
-10
(rad/s)
0
50
100
150
200
250
300
350
400
450
500
(pixel)
0
50
100
(pixel)

(a)

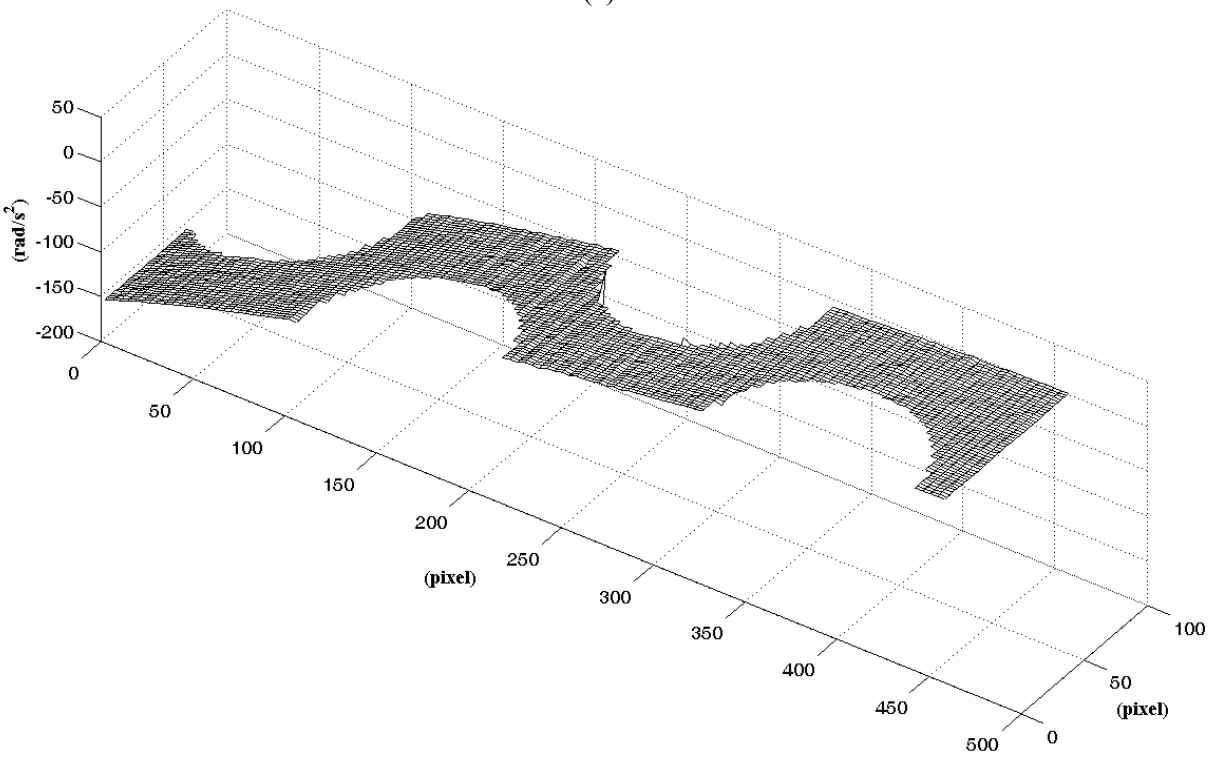
50
0
-50
-100
-150
-200
(rad/s²)
0
50
100
150
200
250
300
350
400
450
500
(pixel)
0
50
100
(pixel)

(b)

Figure 6

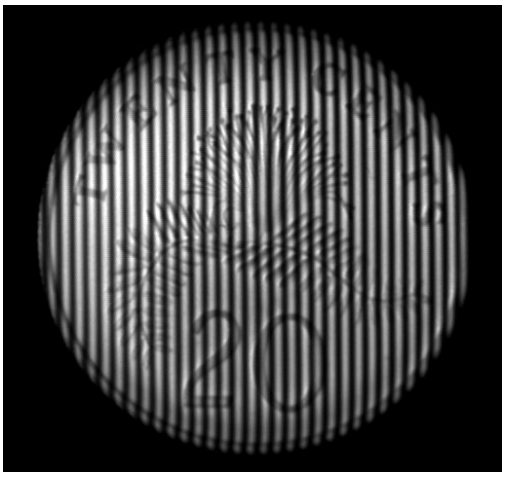

(a)

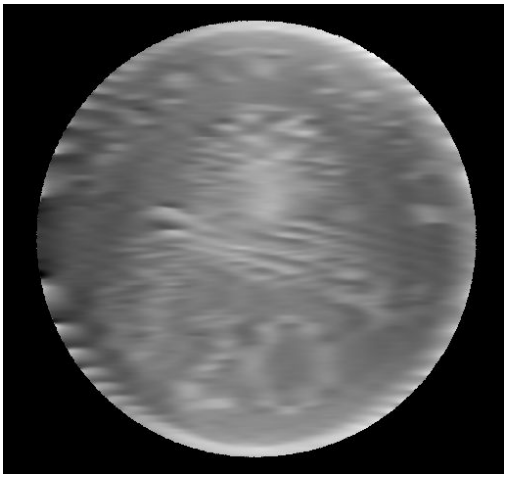

(b)

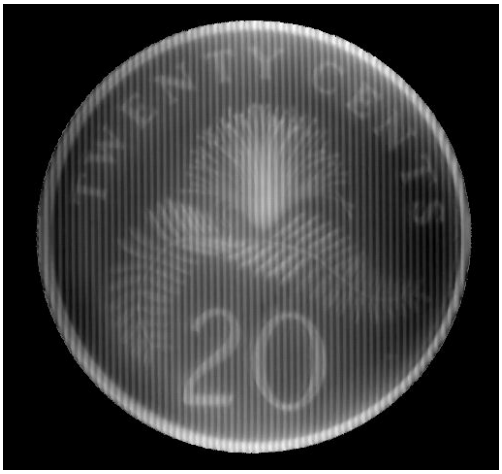

(c)

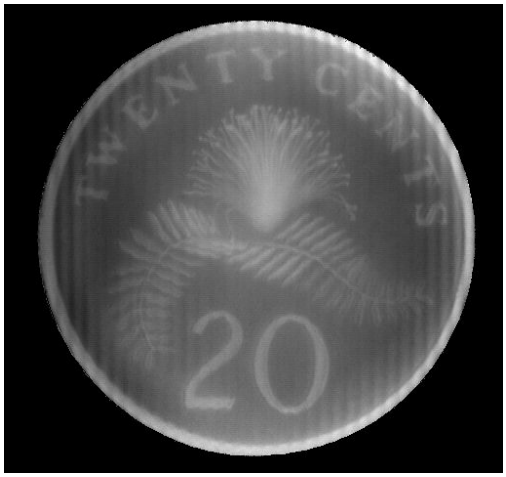

(d)

(e)

(f)

Figure 7